의학석사 학위논문

Secreted Protein Acidic and Rich in Cysteine (SPARC) mediated fluorescence labeled human serum albumin uptake in glioblastoma

악성 뇌교종에서 SPARC 매개에 의한 형광 표지 알부민의 섭취

2017 년 8 월

서울대학교 대학원
협동과정 종양생물학 전공
조 정 환

A thesis of the Degree of Master of Philosophy

악성 뇌교종에서 SPARC 매개에 의한 형광 표지 알부민의 섭취

Secreted Protein Acidic and Rich in Cysteine (SPARC) mediated fluorescence labeled human serum albumin uptake in glioblastoma

August 2017

Interdisciplinary Program in Cancer Biology

Seoul National University

College of Medicine

Jung Hwan Jo

ABSTRACT

Jung Hwan Jo

Interdisciplinary Program in Cancer Biology

The Graduate School

Seoul National University

Objective: Human serum albumin (HSA) is used as a drug carrier for clinical application. Though the mechanism of HSA uptake in tumor is still unclear, it has been known that albumin targets tumor through the leaky blood vessel by enhanced permeability and retention (EPR) effect, indicating that albumin accumulates in tumor by simple infiltration, not by specific uptake. However, it has been suggested that secreted protein acidic and rich in cysteine (SPARC) could sequester albumin in tumor stroma and partly relate to the tumor specific uptake of albumin. For evaluating possible use of HSA as a specific targeting

agent of SPARC-expressing tumor, I visualized SPARC-dependent HSA uptake in glioblastomas.

Methods: Fluorescence labeling, FNR648-N_3 was conjugated to HSA by click chemistry reaction. Human glioblastoma cell line, U87MG, was used for evaluating SPARC-dependant HSA uptake. SPARC expression was down-regulated with shSPARC in U87MG cells. After treatment with FNR648-HSA in U87MG and shSPARC-U87MG, fluorescent signals were measured with confocal microscopy. Colocalization of Cy3-SPARC and FNR648-HSA was observed with confocal FRET analysis. For *in vivo* study, U87MG and shSPARC-U87MG cells were subcutaneously injected to the thighs of a mouse to generate xenograft model. After intravenous injection of FNR648-HSA in a tumor-xenografted mouse, fluorescent signals were detected with IVIS Lumina II. FITC-dextran

was used for vessel permeability test. Immuno-fluorescence staining for tumor frozen section was proceeded with CD31 antibody (for blood vessel) and DAPI (for nucleus). Confocal tile scanning and high resolution imaging were used for detecting fluorescence signal in overall tumor tissue.

Results: SPARC proteins were highly expressed in U87MG, but not in shSPARC-U87MG. *In vitro* HSA uptake test showed that more FNR648-HSA was accumulated in U87MG than shSPARC-U87MG cells. Exogenous SPARC treatment successfully recovered the uptake of FNR648-HSA in shSPARC-U87MG cells. Furthermore, SPARC and HSA were colocalized in U87MG cells. In xenograft model, FNR648-HSA was accumulated 4 times more in U87MG than shSPARC-U87MG. When tumors were detached and compared the difference between them,

though vascular permeability of FITC-dextran in U87MG tumor was similar to shSPARC-U87MG tumor regardless of SPARC expression, more FNR648-HSA was accumulated in U87MG tumor than shSPARC-U87MG tumor. In confocal imaging of tumor section, HSA was escaped from blood vessel and internalized into U87MG tumor cells. On the other hand, HSA was retained in the blood vessel of shSPARC-U87MG tumor.

Conclusion: SPARC have an impact on HSA uptake in glioblastoma. An expression of SPARC increases HSA uptake in a glioblastoma xenografted mouse model. Thus, HSA has a potential for a drug delivery system in SPARC expressing glioblastomas.

Keywords: human serum albumin (HSA), secreted protein acidic and rich in cysteine (SPARC), enhanced

permeability and retention (EPR) effect, dextran, blood permeability, fluorescence imaging, click reaction

Student number: 2015-22064

CONTENTS

LIST OF FIGURES

LIST OF ABBREVIATIONS

SPARC : Secreted Protein Acidic and Rich in Cysteine

HSA : Human Serum Albumin

DBCO-NHS : Dibenzocyclooctyl-NHS

MALDI-TOF : Matrix Assisted Laser Desorption/Ionization

-Time Of Flight

KD : Knock Down

EPR : Enhanced Permeability and Retention

GBM : Glioblastoma Multiform

IVIS : In Vivo Imaging System

FBS : Fetal Bovine Serum

FRET : Fluorescence Resonance Energy Transfer

ROI : Region Of Interest

INTRODUCTION

I. Albumin as an efficient nano particle for clinical applications

Over recent years, one of the main challenges in the field of oncology has been the development of new strategies to improve the effect of anticancer drugs, including the cancer target effect and not damaging normal cells. This is the concept to increase the therapeutic index of the drugs, prolonging their maintenance at the tumor sites and killing the only tumor cells, at the same time reducing their toxic side effects, thus improving the quality of patient's life and overall survival period of patients. Nanomedicine has been developed as one of the most important research in the modern medical science. In particular, the use of nano particles in drug delivery has offered considerable importance for the enhanced

bioavailability of chemotherapeutic agents. Encapsulation within or binding to small colloidal particles may enable drugs to circulate for longer periods of time, to accumulate preferentially within tumor tissue, to have reduced systemic toxicity [1-2].

However, potential toxicity associated with the nano particle itself can be a limitation for clinical applications. There are many causes of nano particle' s potential toxicity including size, shape, charge, compositions, and triggering of immune malfunctions or overreactions. Therefore, it should be carefully considered when selecting the type of carrier for drug transport to the tumor site [3].

In order to overcome these concerns, a feasible approach is to use endogenous proteins inside the human body as drug carriers. So, many endogenous proteins have

been investigated for clinical applications as tumor target imaging or therapy. Among them, Human serum albumin has been used for drug carrier. Albumin is the most abundant blood plasma protein in human. It constitutes 60% total plasma proteins. Albumin' s size is 65~70kDa protein and diameter is 7~8nm. The reasons for using albumin as an versatile tool for drug delivery is based upon its long Half-life in plasma about 19 ~ 20 days. And also the advantages of albumin for clinical application are albumin is easily water-soluble, stable and no toxicity [4-6]. So, albumin is efficient as a drug carrier for tumor imaging and therapy.

II. Tumor-specific targeting with albumin

In previous study, it was reported that there are many ways to transport human serum albumin from vessel to tumor space. First, albumin is non-specifically just

escaped from vessel through leaky junction by EPR effect, indicating that albumin is accumulated in tumor by simple infiltration, not by specific targeting tumor [7-10].

Second, albumin binds to 60 kDa glycoprotein gp60 receptor located on the endothelial cell surfaces in blood vessel and is transported to tumor interstitium by transcytosis and subsequently release the drug into the subendothelial-tumor space [11-13]. Many researchers have thought albumin is almost infiltrated in tumor by EPR effect [7-10, 12]. however, it has been suggested that SPARC present in tumor stroma could sequester albumin in tumor region [14].

Although, many hypothesis of principal albumin's transport have been researched, the scheme how to human serum albumin is accumulated in tumor region still remains to be elucidated. In addition, relationship between SPARC and HSA is not much investigated. So, It is important to

understand SPARC and HSA uptake in tumor cell. In previous Study, In glioblastoma, it was confirmed SPARC expression is high and the SPARC expression is higher in proportion to glioma grade [15]. So, we thought it is clinically important to target imaging of glioblastoma which expresses high SPARC by using albumin.

III. Purpose of this study

In the present study, I investigated the role of SPARC in HSA accumulation, to test the potential of fluorescence labeled HSA as a specific imaging agent for targeting SPARC expressing glioblastoma.

MATERIALS AND METHODS

Cell culture

U251 (glioblastoma), GBM28, GBM37 (glioblastoma primary cancer), MDA MB-231 (breast cancer) were grown in DMEM medium (WELGENE, Gyeongsan, Korea). second, PC3 (prostate cancer), A549 (lung cancer) were grown in RPMI medium (WELGENE, Gyeongsan, Korea), third, U87MG, shSPARC-U87MG, U373 (glioblastoma) were grown MEM medium (Gibco, Grand Island, NY, U.S.A). Each medium (DMEM, MEM, RPMI) contains 10% (v/v) fetal bovine serum (FBS, Gibco, Grand Island, NY, U.S.A) and 1% antibiotics containing penicillin/streptomycin (Invitrogen, Grand Island, NY, U.S.A). Cells were incubated in a 37 ℃ humidified incubator with 5% CO_2 atmosphere.

Cell line establishment

In U87MG, SPARC expression was silenced by SPARC shRNA retroviral transduction. To make almost SPARC knock down U87MG cell line, monoclonal selection was performed. First, SPARC KD U87MG cells (pool) were seeded in 96 well plate (Nalge NUNC International, Naperville, IL, U.S.A; 0.2/well). and then, selected mono cell population in 96 well plate using optical microscope. After proliferated mono cell colonies, mono cell colonies were detached from 96 well plate using trypsin and passed to 6 well plate (Nalge NUNC International, Naperville, IL, U.S.A). Then, also passed to T25 flask or 100ϕ plate.

After proliferating cell in 100ϕ plate, protein was obtained from cell colonies. Then, select almost SPARC knock down U87MG cell line by western blot.

RT-PCR

Total RNA were obtained from cells(U87MG, U7373, U252, GBM28, GBM37, A549, MDA MB-231, PC3) with the Trizol reagent (Invitrogen, CarIsland, CA, U.S.A). For cDNA synthesis, amfiRivert Platinum cDNA synthesis Master Mix(GenDEPOT, Barker,TX, U.S.A) was used with 2 ug of mRNA following the manufacturer' s instructions. From synthesized cDNA, the mRNA expression level of SPARC(secreted protein acidic and rich in cystein) and β-actin were detected. The sequences of the forward and reverse primers of SPARC were 5' -GGT ATC TGT GGG AGC TAA TC-3' and 5' -TCT CAG TCA GAA GGT TGT TG-3' in addition, the sequences of the forward and reverse primers of β-actin were 5' -ACC AGG GCT GCT TTT AAC TCT-3' and 5' -GAG TCC TTC CAC GAT ACC AAA-3' . The PCR was run after an initial single cycle of 94 ℃ for 5 minutes. After initial single cycle,

there are 30 cycles of following procedure; 94 ℃ for 30 seconds, annealing temperature for 1 minute and 72 ℃ for 1 minute. The annealing temperature of SPARC is 53 ℃ and β-actin is 52 ℃. In the last step, 72 ℃ for 10minutes. After amplification, PCR products were analyzed by gel electrophoresis in 1.2% agarose gels and visualized with Loading star(DyneBio Inc, Seoul, Korea) staining

Western blotting

Total proteins were isolated from tumor cells in 4 ℃ condition, using radio-immunoprecipitation assay (RIPA) buffer (Sigma, St. Louis, MO, U.S.A) and protease inhibitor (Roche, Nutley, NJ, Switzerland). Lysates were cleared by centrifugation at 15,000 rpm for 30 minutes at 4℃. Total proteins were quantified by BCA protein assay kit. Lysate of each cell sample (20ug) mixed with 4x polyacrylamide gel electrophoresis sample buffer (Invitrogen, Grand

Island, NY, U.S.A) and 10x sample reducing agent (Invitrogen, Grand Island, NY, U.S.A) was loaded onto 12% SDS-PAGE gel. After gel electrophoresis, the gels protein were transferred onto PVDF membrane (Millipore, Watford, UK). The PVDF membrane was blocked with 5% BSA in Tris-Buffered Saline-Tween20 buffer (20mM Tris, 138mM NaCl and 0.1% Tween20, TBST) for 1 hour at room temperature. The membrane was incubated overnight at 4℃ with primary antibody for SPARC (#5420S, Cell Signaling technology, Danvers, MA, U.S.A; diluted 1:2000 in 0.5% BSA, TBST) and β-actin (A5441, Sigma-Aldrich, St, Louis, MO, U.S.A; diluted 1:5000 in 0.5% Skim milk, TBST). Membrane was then incubated with HRP conjugated anti-rabbit or anti-mouse secondary IgG (cell Signaling Technology, Danvers, MA, U.S.A) for 2 hour at room temperature. Visualization was performed using the ECL reagents (Roche, Nutley, NJ, U.S.A). The signal intensity

was measured using an LAS3000 imaging system (Fujifilm, Tokyo, Japan).

Conjugation of HSA with DBCO and FNR648 fluorescence dye

To obtain FNR648 labeled Human serum albumin, fluorescence dye FNR648-N_3 was used and click chemistry reaction was used to label it into Human serum albumin. First, Human serum albumin (5 mg/ 1 ml in PBS) was mixed with dibenzocycloocytl-NHS ester (DBCO-NHS ester) solution (200ug in DMSO 2ul). Reaction of two molar ratio is HSA : DBCO = 1 : 5.62, Reaction time was 37 ℃, 30 minutes and 4 ℃, overnight. DBCO-HSA conjugates was then purified using PD-10 column (GE Healthcare, little Chalfont, Buckinghamshire, UK) and eluted with the filtered PBS buffer. And the protein concentration was measured by the bicinchoninic acid(BCA)

protein assay kit (Pierce Endogen, Rockford, IL, U.S.A), and the molecular size of sample was analyzed via MALDI-TOF 5800 system (AB SCIEX, Framingham, MA, U.S.A) in every conjugation step. Then, FNR648-N_3 & HSA-DBCO click reaction is 1:1 ratio reaction 4 ℃ incubation overnight. FNR648-HSA conjugates was then purified using PD-10 column (GE Healthcare, little Chalfont, Buckinghamshire, UK) and eluted with the filtered PBS buffer. and the protein concentration was measured by the bicinchoninic acid(BCA) protein assay kit (Pierce Endogen, Rockford, IL, U.S.A), and the molecular size of sample was analyzed via MALDI-TOF 5800 system (AB SCIEX, Framingham, MA, U.S.A).

Confocal imaging

In the *in vitro* cell uptake assay or

immune-fluorescence staining, confocal imaging was used to analyze fluorescence signal in the samples. After finish the *in vitro* cell uptake assay or immune-fluorescence staining, sample was washed with PBS three times. Then, sample was mounted with Prolong Gold reagent (Invitrogen, GrandIsland, NY, U.S.A). and cover the sample with cover slide. The confocal samples were stored at -20 ℃. Fluorescence images were taken by confocal laser scanning microscope (Leica TCS SP8, Wetzlar, Hesse, Germany). Each fluorescence signal was detected in the specific range of wave-length (DAPI; 401-480, FITC; 500-550, TRITC; 580-600, FNR648; 650-750).

In vitro FNR648-HSA cellular uptake assay

In *in vitro* FNR648-HSA cellular uptake test, Human glioblastoma cell line, U87MG cells and

shSPARC-U87MG cells which SPARC shRNA was transducted were seeded in 12 well plate (Nalge NUNC International, Naper ville, IL, U.S.A ; $1x10^5$/well) respectively. The experimental sample groups are divided into 2 groups by cell line according to experimental condition. Cells were incubated in 37 ℃ and incubation times after FNR648-HSA treated were 0.5 hr, 2 hr. Total amount of the treated FNR648-HSA source is 2 nmole/well. After uptake finished, FNR648-HSA source was removed and PBS washing 500 ul/well 2 times. Cell fixation by paraformaldehyde (Santa Cruz biotechnology, Inc, U.S.A ; 300 ul, 10 min/well). and mounting with Prolong Gold reagent (Invitrogen, Grand Island, NY, U.S.A). Total amount of FNR648-HSA cellular uptake is measured by confocal imaging.

Animal xenograft model and *in vivo* imaging

In *in vivo* subcutaneous brain tumor xenograft model in mice, U87MG and shSPARC-U87MG cell line were subcutaneously injected into both thigh leg, $5x10^6$ respectively. tumor size and mice weight were regularly measured in once a week. About 2 weeks later, tumor was formed in both thigh leg and tumor size was measured by caliper. FNR648 labeled HSA (80 ug, 200 ul per mouse) were injected by intravenous injection. After injection, fluorescence signal was measured by IVIS 100 (Total flux>$1x10^6$photon/sec/cm^2/sr). The follow-up time points after dose are 0 hr, 4 hr, 8 hr, 24 hr. Fluorescence signal was taken, after that weight and tumor size of mice were also measured.

Immunofluorescence staining of tumor sections

Xenograft tumors were extracted and were frozen for 24 hours in OCT compound (Leica biosystems, Richmond, IL, U.S.A). After 24 hr, the specimens were cut into 4 ㎛ sections. Frozen tumor section slides were thawed in RT for 5 minutes. Then, washing the slides with PBS for 5 minutes 3times. Then, fixation by paraformaldehyde (Santa Cruz biotechnology, Inc, U.S.A) for 15 minutes. and washing the slides with PBS for 5 minutes 3 times. After washing, permeabilize slide samples with 0.5% Triton X 100 for 15 minutes. after finished permeability step, washing with PBS 3 times and blocked the sample with 10% normal serum, 1% BSA in TBS for 1 hr RT. After blocking, treat the primary antibody diluted 1:100 in 1% BSA, TBS incubated in 4 ℃ overnight. In the following day, incubated samples in RT 1 hr. then, removed the primary antibody and washed with PBS for 5 minutes 3times. Incubated with secondary antibody diluted

1:400 in 1% BSA, TBS for 2 hr RT. after finished incubation, washing with PBS for 5 minutes 3 times then, DAPI staining and mounting. covered sample with coverslide.

Statistical analysis

Results were presented as the mean of percentage standard error. The Mann-Whitney U test was conducted to measure P value. P values < 0.05 were considered to be statistically significant.

RESULTS

Investigation of relationship between SPARC and HSA uptake in several cell lines

To identify the relationship between SPARC and HSA, First, SPARC expression in several cell lines and primary cells was confirmed by RT-PCR and western blot. In glioblastoma, there was high SPARC expression. But, another cell lines express no SPARC (Figure 1(a)). Then, I did *in vitro* albumin uptake test in same cell lines. In all glioblastoma which highly express SPARC protein, it showed much more highly albumin uptake than other cell lines which almost not express SPARC protein (Figure 1(b)). To verify whether SPARC and HSA uptake were correlated, I selected U87MG among the glioblastoma, and I made SPARC knock down U87MG cell line by SPARC

shRNA retro-viral transduction. After that, SPARC protein expression in shSPARC-U87MG pool was confirmed by western blot and it was quantified SPARC expression in shSPARC-U87MG pool was 7 times lower than U87MG's. To obtain U87MG which SPARC is almost not expressed, monoclonal selection was performed using shSPARC-U87MG pool and selected almost SPARC knock down U87MG cell named 1C3. Relative ratio of SPARC protein expression in 1C3 was 74 times lower than U87MG’s (Figure 1(c), Figure 1(d)). Then, experiment proceeded with U87MG and almost SPARC KD U87MG which named 1C3.

.

(a)

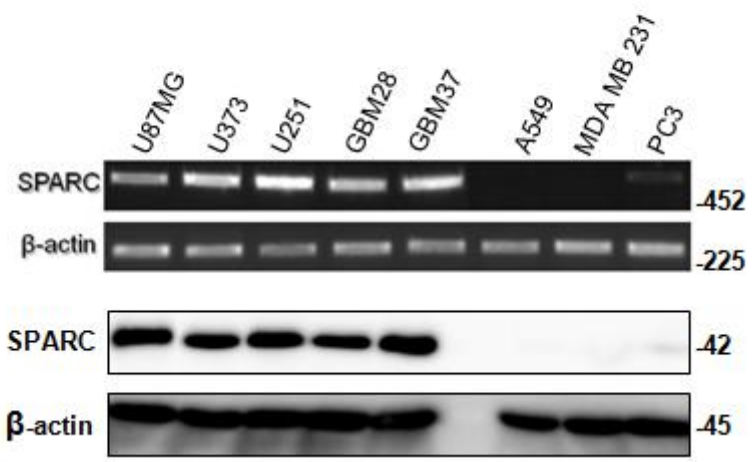
U87MG
U373
U251
GBM28
GBM37
A549
MDA MB 231
PC3
SPARC
β-actin
452
225
SPARC
β-actin
42
45

(b)

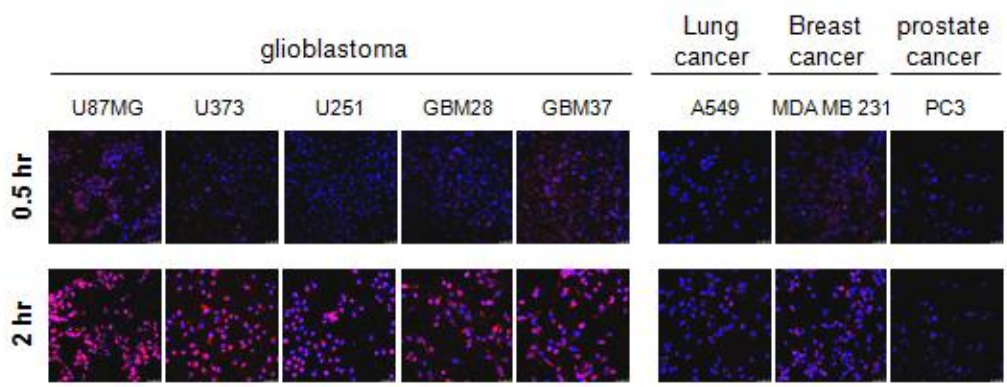
glioblastoma
Lung cancer
Breast cancer
prostate cancer
U87MG
U373
U251
GBM28
GBM37
A549
MDA MB 231
PC3
0.5 hr
2 hr

(c)

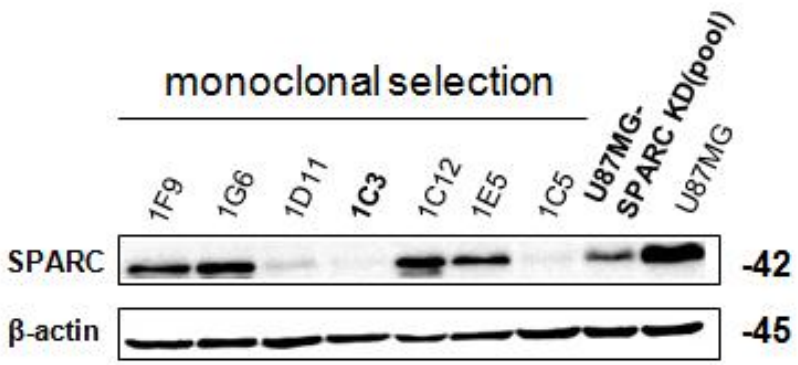
monoclonal selection
1F9
1G6
1D11
1C3
1C12
1E5
1C5
U87MG-SPARC KD(pool)
U87MG
SPARC
β-actin
-42
-45

(d)

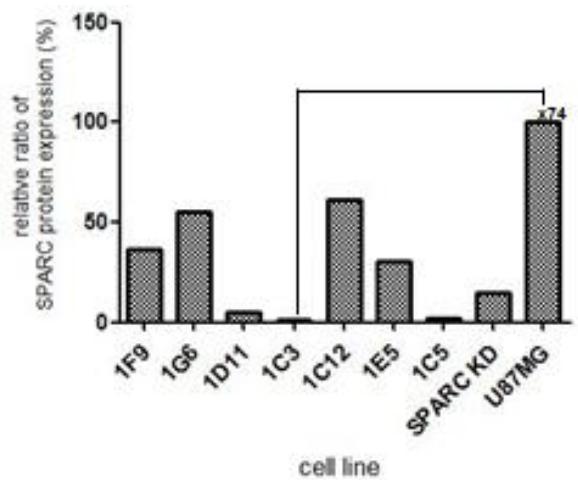
relative ratio of SPARC protein expression (%)
150
100
50
0
x74
1F9
1G6
1D11
1C3
1C12
1E5
1C5
SPARC KD
U87MG
cell line

Figure 1. SPARC expression and albumin uptake in tumor cell lines

(a) In RNA and proteins level, Higher SPARC expression was observed in glioblastoma, but not in other cell lines. SPARC RNA size is 452 bp and β-actin RNA size is 225 bp. SPARC protein size is 42 kDa and β-actin protein size is 45 kDa. (b) In albumin uptake test, SPARC-expressing glioblastomas showed high albumin uptake than other cell lines not expressing SPARC. (c, d) To verify the interaction of SPARC and HSA, U87MG glioblastoma was selected. By SPARC shRNA retro-viral transduction, U87MG cells which show reduced expression of SPARC were generated. As a monoclonal shSPARC-U87MG cells for further research, 1C3 cells were selected among the shSPARC-U87MG. it was confirmed 1C3's SPARC expression was 74 times lower than U87MG's.

Conjugation of HSA and fluorescence dye by click reaction

For making fluorescence labeled Human serum albumin, click chemistry reaction was used. In click reaction, DBCO group and N_3 (azide) group formed covalent bond. First, DBCO-NHS ester bound to HSA. DBCO-NHS conjugated HSA reacts to N_3 (azide) tacking fluorescence dye. Then, Fluorescence dye labeled Human serum albumin was formed by click reaction (Figure 2(a)). After making HSA-DBCO with ratio (HSA : DBCO-NHS=1 : 5.63), it was confirmed 5.4 DBCO-NHS molecules were conjugated to each HSA molecule, measured by MALDI-TOF. Then, After click reaction between HSA-DBCO and FNR648-N_3 with ratio (HSA-DBCO : FNR648-N_3=1 : 5), It was also identified 4.9 FNR648-N_3 molecules bound to each HSA-DBCO molecule (Figure 2(b)).

(a)

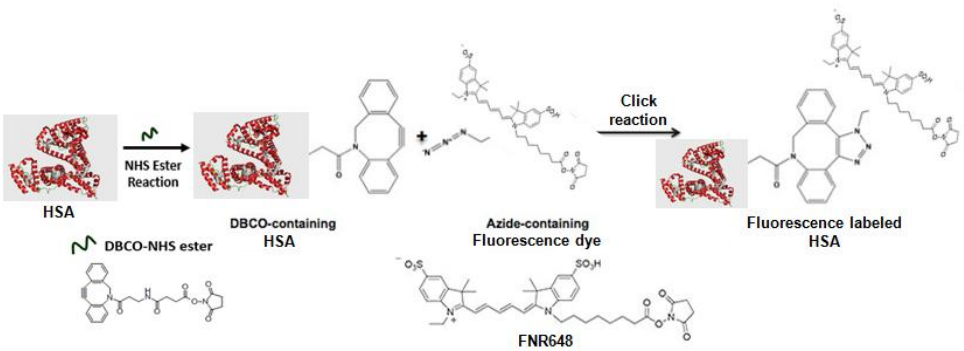

(b)

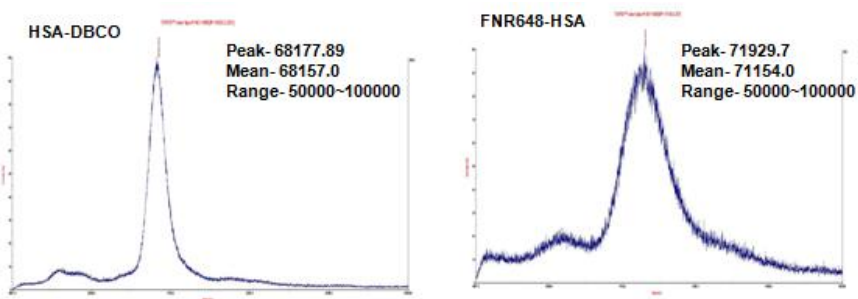

Mw HSA	66213	Mw DBCO-NHS	363.48	Mw FNR648-N_3	766
	Peak	(-HSA)	ratio		
HSA-DBCO	68177.89	1964.89	HSA : DBCO= 1 : 5.4		RXN ratio
FNR648-HSA	71929.7	3751.81	HSA : FNR648-N_3= 1 : 4.9	FNR648: DBCO	0.91: 1

Figure 2. Conjugation of HSA and fluorescence dye by click reaction

(a) Click reaction was used to conjugate Human serum albumin and fluorescence dye. In click reaction, NHS ester group and N_3 azide group formed covalent bond. First, DBCO-NHS ester was bound to HSA. DBCO-NHS conjugated HSA reaction to azide containing fluorescence dye. Then, Fluorescence dye labeled Human serum albumin was formed by click reaction. (b) MALDI-TOF measured how many fluorescence dye molecules bound to human serum albumin. The result showed approximately 5 fluorescence dye molecules are conjugated to one human serum albumin.

Comparison of *in vitro* FNR648-HSA uptake between U87MG and shSPARC-U87MG

In *in vitro* FNR648-HSA cellular uptake assay, we compared the difference of HSA uptake between U87MG and shSPARC-U87MG. First, To see if cells specifically uptake albumin, only FNR648 dye and FNR648-HSA was treated in the cells respectively. the result showed that both cells just only uptake FNR648-HSA, not FNR648 dye. In addition, It was proven that U87MG much more highly uptakes FNR648-HSA compared with shSPARC-U87MG. but, there was very little HSA uptake in shSPARC-U87MG. As the 37 ℃ incubation time is more longer, HSA uptake in U87MG much more increased but, shSPARC-U87MG showed almost no difference in HSA uptake, showing the increased disparity of HSA uptake between two cell lines. Through this result, it was

identified that U87MG much more specifically uptakes albumin than shSPARC-U87MG. To know whether SPARC protein really affects HSA uptake in cell (or not), exogenous SPARC protein was cotreated with FNR648-HSA in U87MG and shSPARC-U87MG. the result showed that shSPARC-U87MG recovered the FNR648-HSA uptake with SPARC protein treatment. U87MG also showed increase of HSA uptake as SPARC was cotreated. But, not glycosylated SPARC protein obtained from E.coli did not function about HSA uptake. Through this result, we knew that HSA uptake was dependent on SPARC protein present and also glycosyl modification is important to SPARC function (Figure 3).

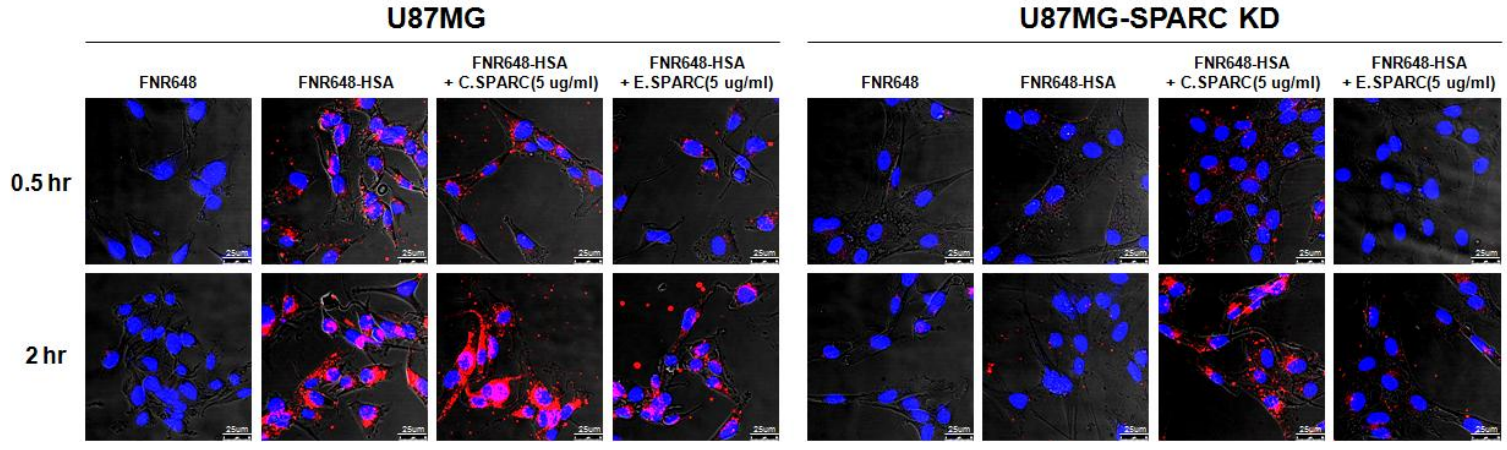
U87MG
U87MG-SPARC KD
FNR648
FNR648-HSA
FNR648-HSA + C.SPARC(5 ug/ml)
FNR648-HSA + E.SPARC(5 ug/ml)
0.5 hr
2 hr

Figure 3. FNR648-HSA uptake in U87MG and shSPARC-U87MG cells

In FNR648-HSA uptake test in U87MG and shSPARC-U87MG, FNR648-HSA was highly accumulated in U87MG cells compared with shSPARC-U87MG. When exogenous SPARC (5ug/ml) was cotreated with FNR648-HSA (2nmole/ml) in U87MG and shSPARC-U87MG, shSPARC-U87MG recovered HSA uptake as SPARC protein was cotreated. U87MG also showed increase of HSA uptake with exogenous SPARC treatment.

In vitro SPARC and HSA colocalization in glioblastoma

To identify whether SPARC and HSA were colocalized in the cell, *In vitro* colocalization test was performed in U87MG and shSPARC-U87MG. SPARC protein was labeled with Cy3 fluorescence dye while, HSA was labeled with FNR648 fluorescence dye. the result was that when just only FNR648-HSA was treated in the cells, FNR648-HSA was much more highly accumulated in U87MG cells than shSPARC-U87MG likewise. After that, when not labeled SPARC and FNR648-HSA were cotreated in the cells, shSPARC-U87MG recovered FNR648-HSA uptake much highly. So, we treated just only Cy3-SPARC protein in both cells and Cy3-SPARC was very well internalized in both. According to this result, when Cy3-SPARC and FNR648-HSA were cotreated together,

The result showed that Cy3-SPARC and FNR648-HSA were all internalized and existed as a colocalized form in both cell's cytoplasm (Figure 4(a)). To compare signal match between Cy3-SPARC and FNR648-HSA, line ROI analysis was used and it showed Cy3-SPARC and FNR648-HSA were almost matched (Figure 4(b)).

To prove more accurately, FRET analysis was utilized with confocal, z-stack and 3D imaging technique. The data showed Cy3-SPARC and FNR648-HSA were completely colocalized in the cells (Figure 4(c, d, e)). FRET line ROI analysis also verified Cy3-SPARC and FNR648-HSA were all matched (Figure 4(f)). Through these several results, it was supposed that there is relationship between SPARC and HSA.

(a)

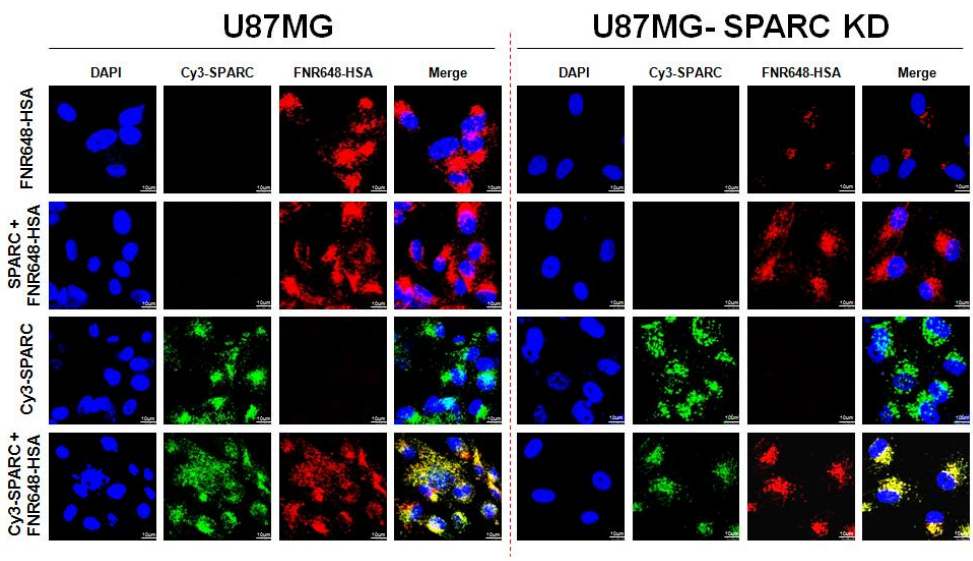
U87MG
U87MG- SPARC KD
DAPI
Cy3-SPARC
FNR648-HSA
Merge
FNR648-HSA
SPARC + FNR648-HSA
Cy3-SPARC
Cy3-SPARC+ FNR648-HSA

(b)

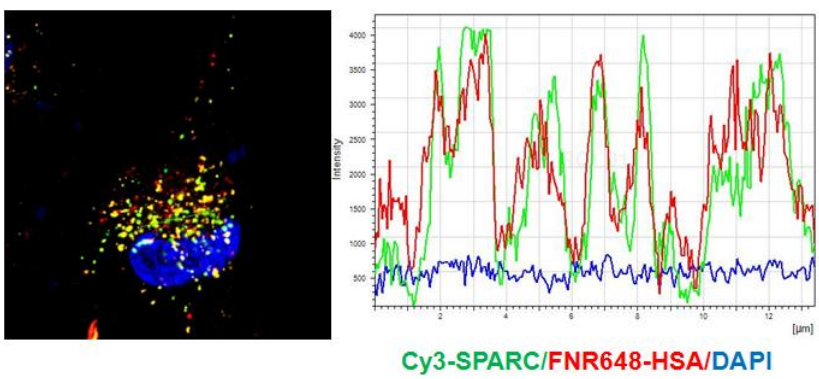
Intensity
[µm]
Cy3-SPARC/FNR648-HSA/DAPI

(C)

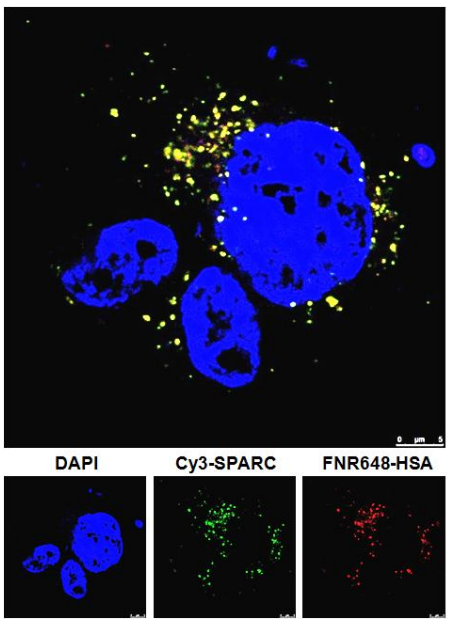

(d)

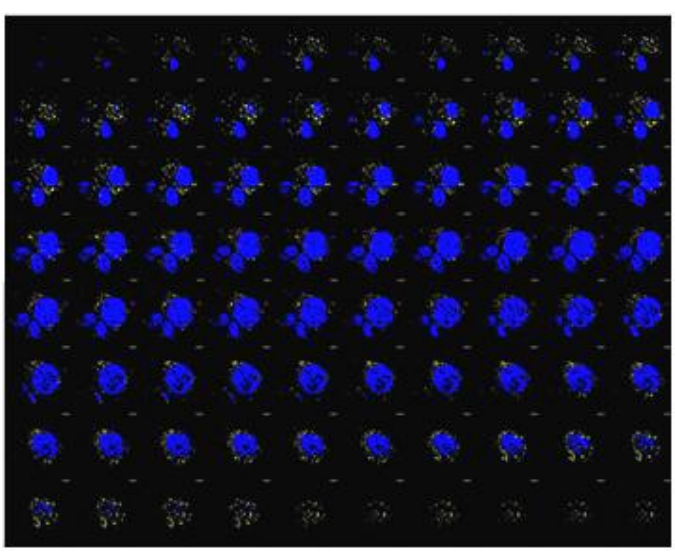

(e)

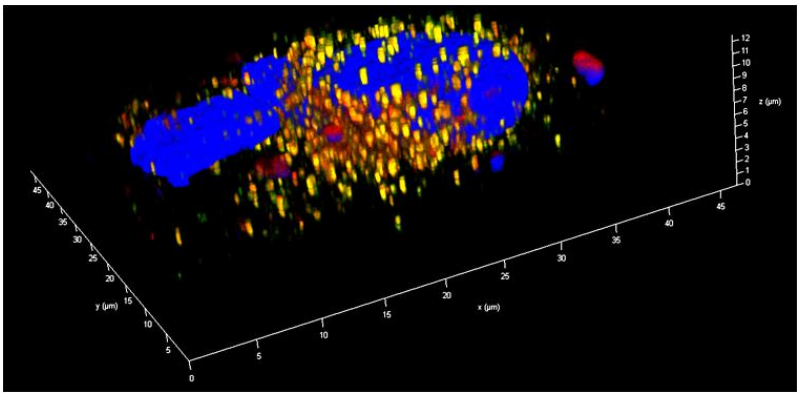

(f)

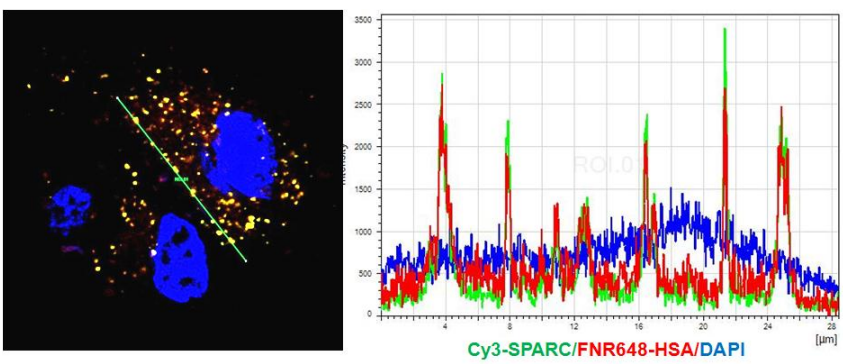

Figure 4. Cy3-SPARC and FNR648-HSA colocalization in U87MG cells

(a) In colocalization, SPARC protein was labeled with Cy3 fluorescence dye while, HSA was labeled with FNR648 fluorescence dye by click reaction. Cy3-SPARC and FNR648-HSA were all internalized in addition, existed as a colocalized form in U87MG and shSPARC-U87MG. Cy3-SPARC's fluorescence color is green, FNR648-HSA's fluorescence color is red. (b) line ROI analysis showed Cy3-SPARC and FNR648-HSA were almost matched. (c, d, e) FRET analysis using high resolution confocal, z-stack and 3D imaging showed Cy3-SPARC and FNR648-HSA were completely colocalized in the cells. (f) FRET line ROI analysis also verified Cy3-SPARC and FNR648-HSA were all matched.

In vivo fluorescence imaging of FNR648-HSA in U87MG and shSPARC-U87MG tumor model

To verify whether this relationship between SPARC and HSA uptake is also identified at *in vivo* study, For xenograft model, U87MG and shSPARC-U87MG were subcutaneously injected into both thigh legs, respectively (Figure 5(a)) and after tumor grew, we selected U87MG and shSPARC-U87MG almost same size tumor models and injected FNR648-HSA through tail vein (Figure 5(b)). During the 5 min, 4, 8, 24 hr follow-up, Serial fluorescence imaging revealed that FNR648-HSA was more highly accumulated in U87MG tumor than shSPARC-U87MG tumor (Figure 5(c)). HSA accumulation in U87MG tumor increased and retained gradually until 4 hr. At 4 hr, HSA is most accumulated in U87MG tumor region and 4 times higher uptake than shSPARC-U87MG

tumor. As time flow after 4 hr, HSA was gradually excreted from body and tumor. At 24 hr, the *in vivo* tumor imaging difference between U87MG and shSPARC-U87MG tumor is more apparent than any other time-point, showing 6 times higher HSA uptake in U87MG tumor than shSPARC-U87MG's. On the other hand, shSPARC-U87MG almost didn't show HSA accumulation in tumor (Figure 5(d)).

(a)

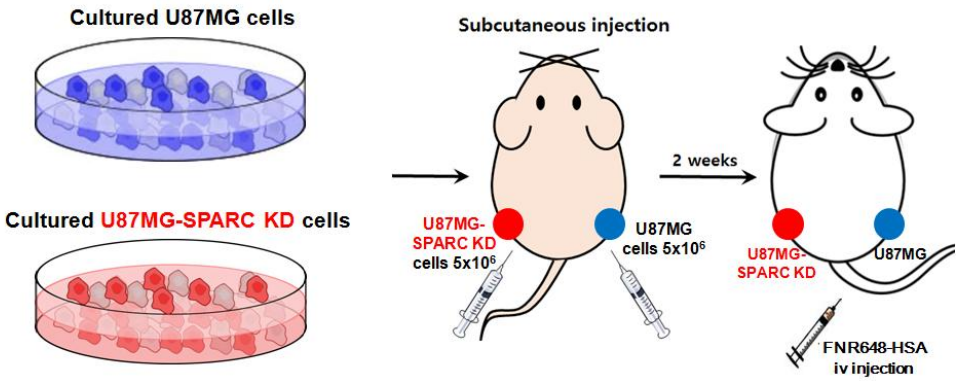
Cultured U87MG cells
Cultured U87MG-SPARC KD cells
Subcutaneous injection
U87MG-SPARC KD cells 5x10^6
U87MG cells 5x10^6
2 weeks
U87MG-SPARC KD
U87MG
FNR648-HSA iv injection

(b)

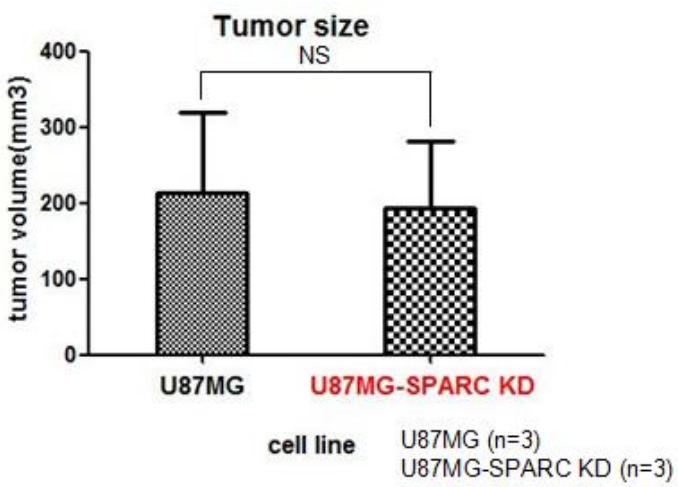
Tumor size
NS
tumor volume(mm3)
400
300
200
100
0
U87MG
U87MG-SPARC KD
cell line
U87MG (n=3)
U87MG-SPARC KD (n=3)

(c)

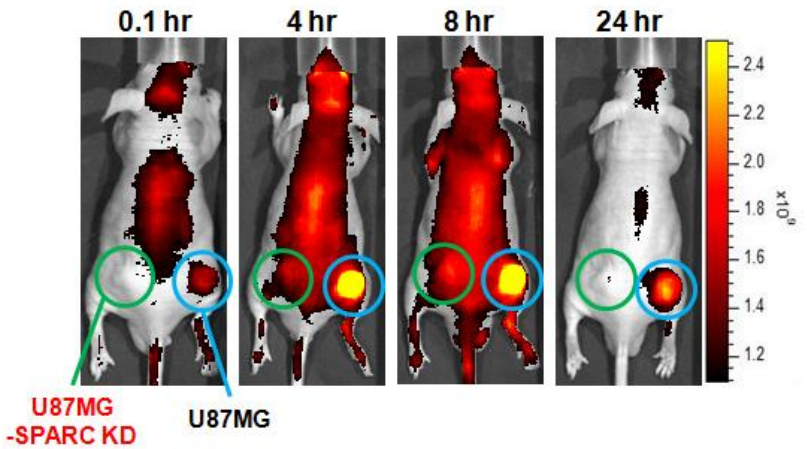
0.1 hr
4 hr
8 hr
24 hr
2.4
2.2
2.0
1.8
1.6
1.4
1.2
x10⁹
U87MG
-SPARC KD
U87MG

(d)

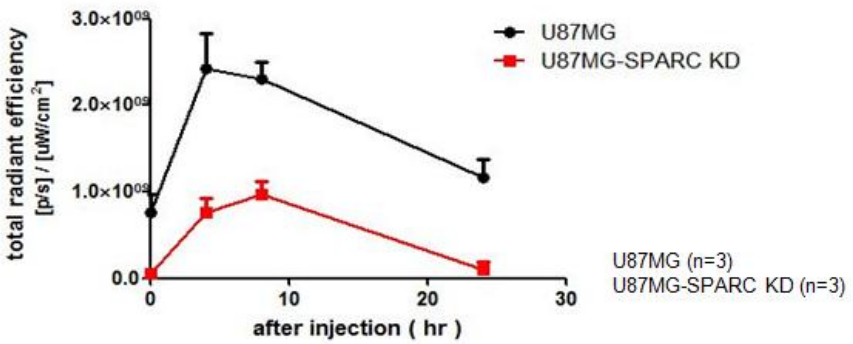
3.0×10⁰⁹
2.0×10⁰⁹
1.0×10⁰⁹
0.0
total radiant efficiency
[p/s] / [uW/cm²]
0
10
20
30
after injection (hr)
U87MG
U87MG-SPARC KD
U87MG (n=3)
U87MG-SPARC KD (n=3)

Figure 5. FNR648-HSA imaging in U87MG, shSPARC-U87MG tumor model

(a) U87MG and shSPARC-U87MG cells were subcutaneously injected into both thigh legs, $5x10^6$ respectively. (b) U87MG and shSPARC-U87MG almost same size tumor models were selected and injected FNR648-HSA through tail vein. NS, non-significant difference. (C) Serial fluorescence imaging revealed that FNR648-HSA was more highly accumulated in U87MG tumor than shSPARC-U87MG tumor. (d) At 4 hr, HSA is most accumulated in U87MG tumor region and 4 times higher uptake than shSPARC-U87MG tumor. At 24 hr, the *in vivo* tumor imaging difference between U87MG and shSPARC-U87MG tumor is more apparent, showing 6 times higher HSA uptake in U87MG than shSPARC-U87MG's.

Biodistribution & *ex vivo* imaging of FITC-dextran and FNR648-HSA in tumor model

To confirm the difference of vessel infiltration rate and EPR effect between U87MG and shSPARC-U87MG tumor, FNR648-HSA and FITC-dextran which is same size of HSA were used and coinjected into tumor model by tail vein. In biodistribution of tumor model for 1, 4, 8, 24 hr time point, U87MG tumor is more highly uptake of FNR648-HSA & FITC-dextran than shSPARC-U87MG's at all time points. As time flow, albumin, dextran was metabolized in liver and excreted through the GI tract. However, much albumin was left in U87MG tumor region although dextran was excreted as time flow (Figure 6(a)). After that, we detached the tumors at each time point 1 hr, 4 hr, 8 hr, 24 hr respectively. In *ex vivo* imaging of

FITC-dextran and FNR648-HSA in U87MG and shSPARC-U87MG tumor, FNR648-HSA was more highly accumulated in U87MG tumors than shSPARC-U87MG tumor in the same manner. in case of dextran, FITC-dextran was a little more infiltrated into U87MG tumor than shSPARC-U87MG's but, not very big difference. as time flow, FITC-dextran was not accumulated but very rapidly excreted from both tumors, whereas, FNR648-HSA was highly accumulated and retained in U87MG tumor (Figure 6(b)).

(a)

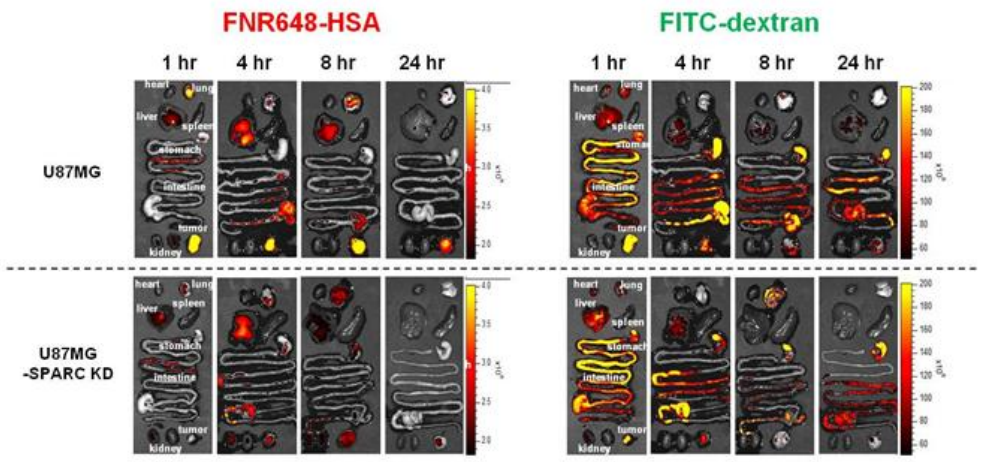
FNR648-HSA
FITC-dextran
1 hr
4 hr
8 hr
24 hr
U87MG
U87MG
-SPARC KD
heart
lung
liver
spleen
stomach
intestine
tumor
kidney

(b)

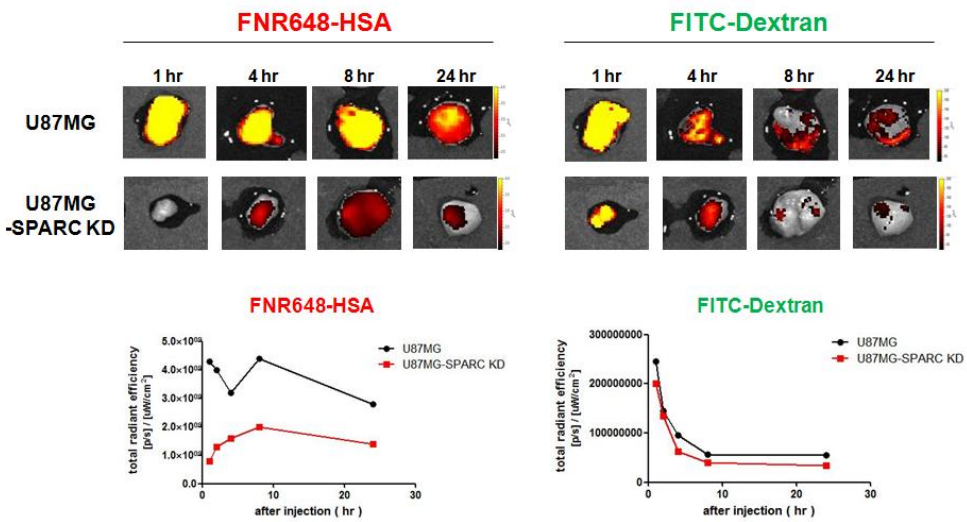
FNR648-HSA
FITC-Dextran
1 hr
4 hr
8 hr
24 hr
U87MG
U87MG
-SPARC KD
FNR648-HSA
FITC-Dextran
U87MG
U87MG-SPARC KD
total radiant efficiency
[p/s] / [uW/cm²]
after injection (hr)

Figure 6. FNR648-HSA, FITC-dextran imaging in U87MG, shSPARC-U87MG tumor

(a) FNR648-HSA and FITC-dextran which is same size of HSA were used and coinjected into tumor model by tail vein. In biodistribution of tumor model for 1, 4, 8, 24 hr time point, U87MG tumor is more highly uptake of FNR648-HSA & FITC-dextran than shSPARC-U87MG's at all time points. As time flow, albumin, dextran was metabolized in liver and excreted through the GI tract. However, much albumin was left in U87MG tumor region although dextran was excreted as time flow. (b) In *ex vivo* imaging of FITC-dextran and FNR648-HSA in U87MG and shSPARC-U87MG tumor, FNR648-HSA was more highly accumulated in U87MG tumor than shSPARC-U87MG tumor in the same manner. in case of dextran, FITC-dextran was a little more infiltrated into U87MG tumor than

shSPARC-U87MG's but, not very big difference between them. As time flow, FITC-dextran was not accumulated but very rapidly excreted from both tumors, whereas, FNR648-HSA was highly accumulated and retained in U87MG tumor.

Comparison of FNR648-HSA and FITC dextran's infiltration in tumor region between U87MG and shSPARC-U87MG

we did Immuno-fluorescence staining and confocal imaging with tumor frozen section which is 4 hr follow-up of HSA uptake. Through the confocal tile scan of whole tumor tissue, we identified FNR648-HSA was accumulated in the overall U87MG tumor region, but, shSPARC-U87MG tumor region almost did not show FNR648-HSA accumulation. Using the high resolution confocal imaging, Albumin was more infiltrated into tumor space in U87MG tumor than shSPARC-U87MG tumor tissue. in addition, U87MG cells uptake albumin also identified. On the other hand, In shSPARC-U87MG tumor, albumin and dextran was not infiltrated from the tumor vessel and excreted from tumor (Figure 7).

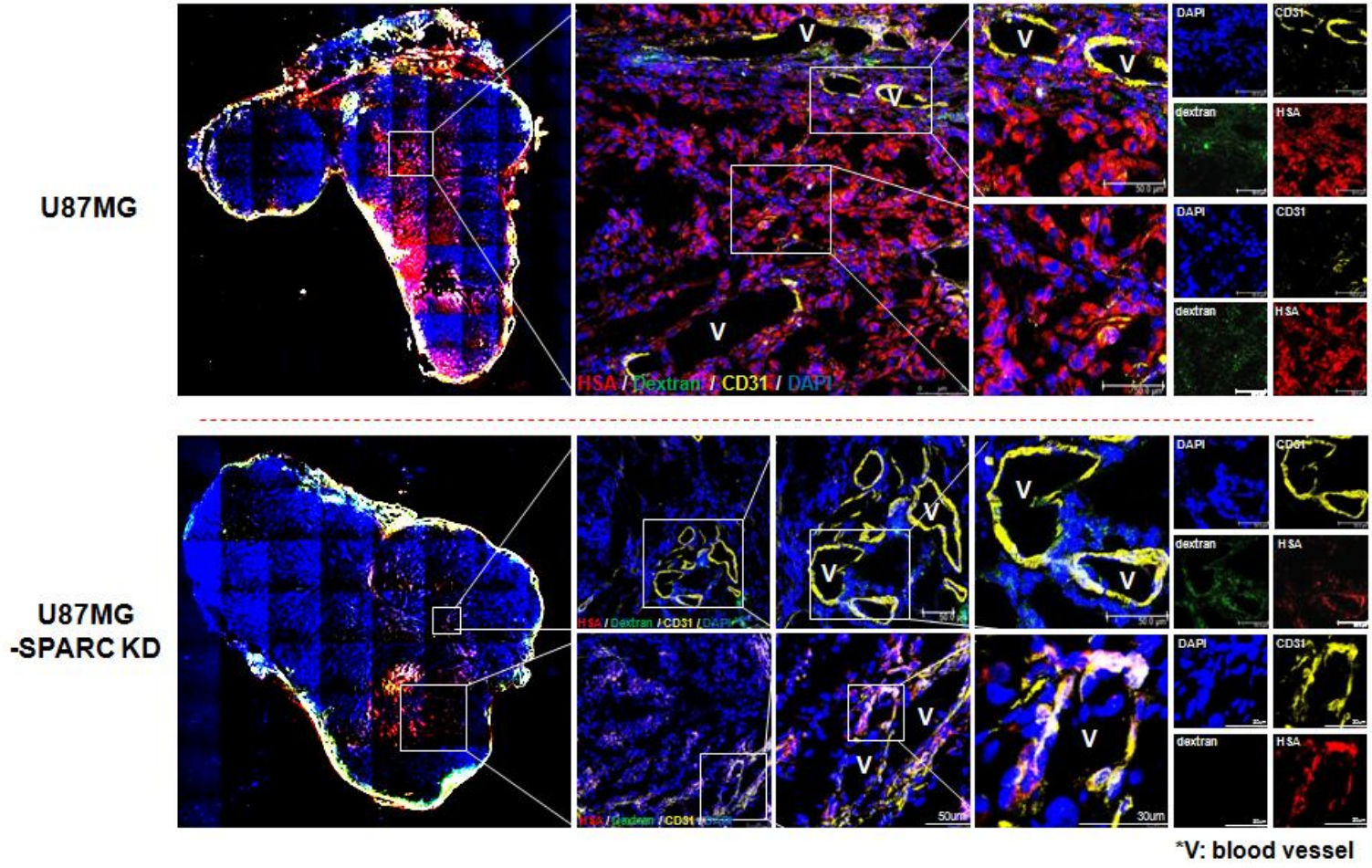
U87MG
U87MG
-SPARC KD
V
HSA / Dextran / CD31 / DAPI
DAPI
CD31
dextran
HSA
50um
30um
*V: blood vessel

Figure 7. Confocal imaging of FNR648-HSA and FITC-Dextran's Infiltration in tumor region

Immuno-fluorescence staining and confocal imaging was proceeded with tumor frozen section which is 4 hr follow-up of HSA uptake in U87MG, shSPARC-U87MG model. Blood vessel was stained by CD31 antibody, and cell nucleus was stained with DAPI.

DISCUSSION

In this study, various glioblastomas have a high SPARC expression. besides, through the primary cell 's western blot, it was proved SPARC expression is higher in proportion to glioma grade as reported [15]. It was first visualized *In vitro* HSA uptake in several cell lines. The result was that In all glioblastomas which highly expressed SPARC, it showed more albumin uptake than other cell lines which almost not expressed SPARC. Furthermore, when compared the difference between same glioblastoma patient's primary cell GBM28 and GBM37, GBM37 which is more malignant than GBM28 expressed more SPARC protein than GBM28 and GBM37 showed more albumin uptake than GBM28. Through this result, it was thought that relation between SPARC and albumin is clinically important to investigate tumor target therapy

using albumin. When compared HSA uptake between U87MG and shSPARC-U87MG, U87MG showed higher HSA uptake than shSPARC-U87MG. In addition, *in vitro* HSA uptake of shSPARC-U87MG was recovered by exogenous SPARC treatment. Taken together overall these results, SPARC works on HSA uptake in tumor cells.

To identify How SPARC and HSA were related in the cell, *in vitro* colocalization test in U87MG and shSPARC-U87MG was performed. Using FRET, it was identified SPARC and HSA were all internalized and existed as a colocalized form in both cells. Therefore, it was proved that there is correlation between SPARC and HSA. In other study, it was also showed SPARC and BSA were colocalized, likewise. Furthermore, binding between SPARC and BSA was proved by immunoprecipitation and SPR [16].

To confirm whether this SPARC effect on HSA uptake was also identified in *in vivo* study, Tumor imaging of FNR648-HSA proceeded and HSA was more accumulated in U87MG tumor than shSPARC-U87MG tumor. To compare the difference of vessel infiltration rate and EPR effect between U87MG and shSPARC-U87MG tumor, FITC-dextran and FNR648-HSA were coinjected in both tumor model. the result showed that FNR648-HSA was more accumulated in U87MG tumors than shSPARC-U87MG tumor, likewise. In case of dextran, FITC-dextran was a little more infiltrated into U87MG tumor than shSPARC-U87MG's but, not very big difference. In other paper, it was referred SPARC could make vessel more permeable by controling endothelial intercellular junction through the VCAM1 signaling [17-21]. However, much albumin was retained in U87MG tumor region, although dextran was rapidly excreted from tumor as time flow.

Through this result, it was supposed that main cause of HSA uptake in tumor is not just EPR effect but also, SPARC have an impact on HSA uptake in tumor.

Confocal imaging of tumor section also supported that HSA accumulation in tumor region was dependent on SPARC present. For the further study, SPARC methylation frequently rose in many other cancers like a colorectal cancer, gastric cancer, pancreatic adenocarcinoma and so on. This SPARC methylation contributes to cancer patient's poor survival [22-24]. So, it is clinically important to investigate albumin mediated drug's tumor target efficiency and therapeutic effect as making SPARC de-methylation in other cancers which SPARC was hyper-methylated. Besides, as making orthotopic tumor models which one shows high SPARC expression and the other shows no SPARC expression, it is important to evaluate correlation effect between SPARC and albumin's

tumor target efficiency in tumor origin microenvironment. So, it can be approximatively estimated albumin's tumor target efficiency value in cancer patients depending on tumor's SPARC expression.

In conclusion, It was successfully visualized SPARC have an impact on HSA uptake in glioblastoma. Therefore, it is supposed that fluorescence labeled HSA is an efficient imaging agent to target SPARC expressing tumors with enormous potential. In addition, HSA is clinically worth of delivering drug system in glioblastoma, according to glioblastoma's SPARC expression.

REFERENCES

[1] Brigger I, Dubernet C, Couvreur P. Nanoparticles in cancer therapy and diagnosis. Adv Drug Deliv Rev. 54:631-51 (2002).

[2] Dobrovolskaia, M. A., & McNeil, S. E. Immunological properties of engineered nanomaterials. Nature Nanotechnology. 2(8), 469-478 (2007).

[3] Singh S, Sharma A, Robertson GP. Realizing the clinical potential of cancer nanotechnology by minimizing toxicologic and targeted delivery concerns. Cancer Res. 72:5663-8 (2012).

[4] Matsumura Y, Maeda H. A new concept for macromolecular therapeutics in cancer chemotherapy: mechanism of tumoritropic accumulation of proteins and

the antitumor agent smancs. Cancer Res. 46:6387-92 (1986).

[5] Kratz, F. Albumin as a drug carrier: Design of prodrugs, drug conjugates and nanoparticles. Journal of Controlled Release. 132(3), 171-183 (2008).

[6] Elzoghby, A. O., Samy, W. M., & Elgindy, N. a. Albumin-based nanoparticles as potential controlled release drug delivery systems. Journal of Controlled Release. 157(2), 168-182 (2012).

[7] Langer, K., Balthasar, S., Vogel, V., Dinauer, N., Von Briesen, H., & Schubert, D. Optimization of the preparation process for human serum albumin (HSA) nanoparticles. International Journal of Pharmaceutics. 257(1-2), 169-180 (2003).

[8] Owens, D. E., & Peppas, N. A. Opsonization, biodistribution, and pharmacokinetics of polymeric

nanoparticles. International Journal of Pharmaceutics, 307(1), 93-102 (2006).

[9] Vonarbourg, A., Passirani, C., Saulnier, P., & Benoit, J.-P. Parameters influencing the stealthiness of colloidal drug delivery systems. Biomaterials. 27(24), 4356-4373 (2006).

[10] Prabhakar, U., Maeda, H., Jain, R. K., Sevick-Muraca, E. M., Zamboni, W. Farokhzad, O. C., et al. Challenges and key considerations of the enhanced permeability and retention effect for nanomedicine drug delivery in oncology. Cancer Research. 73(8), 2412-2417 (2013).

[11] Fanciullino, R., Ciccolini, J., & Milano, G. Challenges, expectations and limits for nanoparticles-based therapeutics in cancer: A focus on nano-albumin-bound drugs. Critical Reviews in Oncology/Hematology. 88, 504--513 (2013).

[12] Li, C., Li, Y., Gao, Y., Wei, N., Zhao, X., Wang, C., et al. Direct comparison of two albumin-based paclitaxel-loaded nanoparticle formulations: Is the crosslinked version more advantageous? International Journal of Pharmaceutics. 468(1-2), 15-25 (2014).

[13] Tiruppathi, C., Song, W., Bergenfeldt, M., Sass, P., & Malik, A. B. Gp60 activation mediates albumin transcytosis in endothelial cells by tyrosine kinase-dependent pathway. The Journal of Biological Chemistry, 272(41), 25968--25975 (1997).

[14] Ma, P., & Mumper, R. J. Paclitaxel nano-delivery systems: A comprehensive review Journal of Nanomedicine and Nanotechnology, 4(2), 1000164 (2013).

[15] Andrei T., Davide M., Antonio G. N., Vincent C. Sparc-Like Protein 1 Is a New Marker of Human Glioma Progression. J. Proteome Res. 11 (10), 5011-5021 (2012).

[16] Alexandre C., Marija D., Helen R. S., Mark A., Lisa J. G., Ryan M., Gillian D., Jeremy D. M., Susan L. C. Secreted protein acidic and rich in cysteine (SPARC) induces lipotoxicity in neuroblastoma by regulating transport of albumin complexed with fatty acids. oncotarget. 7 (47), 77696-77706 (2016).

[17] Reymond, N., d'Agua, B. B & Ridley, A.J. Crossing the endothelial barrier during metastasis. Nat. Rev. Cancer 13, 858-870 (2013).

[18] Kelly, K. A. et al. SPARC is a VCAM-1 counter-ligand that mediates leukocyte transmigration. J. Leukoc. Biol. 81, 748-756 (2007).

[19] Butcher, E. C. Leukocyte-endothelial cell recognition: three (or more) steps to specificity and diversity. Cell. 67, 1033-1036 (1991).

[20] Elices, M. J. et al. VCAM-1 on activated endothelium

interacts with the leukocyte integrin VLA-4 at a site distinct from the VLA-4/fibronectin binding site. Cell. 60, 577-584 (1990).

[21] Klemke, M., Weschenfelder, T., Konstandin, M. H. & Samstag, Y. High affinity interaction of integrin alpha4beta1(VLA-4) and vascular cell adhesion molecule 1 (VCAM-1) enhances migration of human melanoma cells across activated endothelial cell layers. J. Cell. Physiol. 212, 368-374 (2007).

[22] Eungi Y., Hyun J. K., Kwi H. K. Frequent inactivation of SPARC by promoter hypermethylation in colon cancers. Int. J. Cancer: 121, 567--575 (2007).

[23] Norihiro S., Noriyoshi F., Naoki M. SPARC/osteonectin is a frequent target for aberrant methylation in pancreatic adenocarcinoma and a mediator of tumor-stromal interactions Oncogene. 22, 5021--5030

(2003)

[24] Nagaraju, El-Rayes BF. SPARC and DNA methylation: possible diagnostic and therapeutic implications in gastrointestinal cancers. Cancer Lett.1;328(1):10-7 (2013).

국문초록

목적: 사람혈청알부민은 임상에서 약물을 나르는 운반체 또는 방사선 동위원소가 표지된 치료물질로 사용된다. 종양 내 알부민의 유입 기전은 아직 불분명하나, 그동안, 알부민은 누출하는 혈관으로 인해 비특이적으로 종양 쪽으로 빠져나가 쌓이는 EPR 효과로 종양을 표적한다는 것이 알려져 왔다. 그러나 최근 암에서 분비하는 SPARC이라는 물질이 알부민을 종양 내로 끌어들일 수 있고 부분적으로 종양 내 알부민의 특이적 유입과 관련되어 있다고 제시되었다. 따라서 본 연구에서는 악성 뇌교종에서 SPARC의 역할이 알부민 유입과 어떠한 연관성이 있는지를 연구하였다.

방법: 형광물질인 FNR648-N_3를 사람혈청알부민에 click화학반응을 통해 표지하였다. SPARC 의존적 알부민 유입효과를 평가하기 위해 사람 악성 뇌교종 세포주인 U87MG가 사용되었다. U87MG에 SPARC shRNA를 사용하여 SPARC 발현이 감소한 세포주를 구축하였다. U87MG와 shSPARC-U87MG에 FNR648이 표지된 알부민을 처리

하고 난 후, 형광 신호를 공초점 현미경으로 측정하였다. U87MG와 shSPARC-U87MG에서 Cy3-SPARC 과 FNR648-HSA 간의 결합을 FRET 기법을 통해 확인하였다. *in vivo* 연구를 위해, U87MG와 shSPARC-U87MG 세포들을 동물 피하에 주입하여 종양모델을 제작하였다. 종양 모델에 FNR648이 표지된 알부민을 꼬리정맥 주사를 통해 주입하고 난 후, 형광 신호를 IVIS Lumina II를 통해 검출하였다. 종양 조직 절단 샘플을 가지고 면역 형광 염색을 진행하였다. 종양 내 혈관은 CD31 항체를 가지고 염색하였고 그리고 세포핵은 DAPI로 염색되었다. 종양 조직 전반 내 형광 신호를 탐지하기 위해 공초점 조직 주사 영상과 고해상도 공초점 현미경 영상이 사용되었다.

결과: U87MG 세포에서 SPARC 단백질이 높게 발현한 반면, shSPARC-U87MG 세포에서는 SPARC 단백질이 발현하지 않았다. *In vitro* 알부민 uptake 실험에서 U87MG가 shSPARC-U87MG 세포에 비해 훨씬 더 세포 내에 FNR648가 표지된 알부민이 축적되는 결과를 보였다. 외부에서 SPARC 단백질의 처리는 성공적으로 shSPARC-U87MG 세포로 하여금 FNR648이 표지된 알부민의 흡수

를 회복시켰다. 게다가, FRET을 이용하여 SPARC과 알부민이 U87MG 세포 내에서 같이 결합한 형태로 존재함을 확인하였다. 종양 모델에서 shSPARC-U87MG 종양에 비해 U87MG 종양에 훨씬 더 많은 FNR648-알부민이 축적되었고 이는 4배 더 높은 축적정도 차이를 보였다. 종양 혈관 투과정도 비교 실험을 위해 FITC가 표지된 덱스트란이 사용되었으며, 이는 U87MG 종양이 shSPARC-U87MG 종양에 비해 상대적으로 좀 더 높은 혈관 투과성을 보여주었다. 그러나 종양 간 혈관 투과성 차이는 크게 차이 나지 않았다. FITC-덱스트란은 점진적으로 모든 종양에서 배출된 반면, FNR648-알부민은 U87MG 종양에 높게 축적되었다. 하지만, shSPARC-U87MG 종양은 그러지 않았다. 종양 절단 조직 공초점 영상에서 알부민은 U87MG 종양에서 shSPARC-U87MG 종양에 비해 훨씬 더 많이 투과되고 U87MG 종양세포에 섭취된 반면, shSPARC-U87MG 종양에서는 알부민이 투과되지 못하고 혈관에 갇혀 빠져나가지 못하였다.

결론: 악성 뇌교종에서 SPARC이 과발현함을 확인하였고 형광 표지 알부민은 SPARC 의존적으로 악성 뇌교종에 표적하였다. 알부민은

SPARC을 과발현하는 악성 뇌교종을 표적하는 약물전달체로서 잠재성이 있다.

핵심어: 사람 혈청 알부민, SPARC, EPR 효과, 덱스트란, 혈관 투과성, 형광 영상, click 화학 반응

학번: 2015-22064